ABSTRACT

Plant simulation models are abstractions of plant physiological processes. They are useful for investigating the responses of plants to changes in their environment and physical structure. Photosynthesis is a basic plant process that drives growth and biomass accumulation. Thus the simulation of photosynthetic processes is a basic requirement for any plant simulation model. The objective of this work is to develop and document a computer software module that encapsulates equations and parameters to simulate the process of light capture, gas exchange of CO_2 and water vapor, and production of carbohydrate by a plant leaf. The module is written in C++. The program simulates leaf gas exchange processes by coupling photosynthesis with leaf energy balance through stomatal conductance for both C_3 and C_4 crops. The coupled-model approach can describe the photosynthetic behavior of leaves by taking into account the biochemical limitation for CO_2 assimilation (demand) as well as the stomatal limitation to the supply of CO_2, linked to transpiration and canopy temperature. The module's input and output data are documented and complete, compilable code is presented along with a simple interface written in C# to interact with the module. The environmental input required by the module includes net radiation, ambient air temperature, relative humidity, and atmospheric CO_2 concentration. The module outputs transpiration rate, net and gross CO_2 assimilation rates, respiration rate, leaf temperature, internal CO_2 concentration and stomatal conductance. Measured photosynthesis data and parameters for maize, potato and rose are also presented to allow evaluation of the gas exchange simulations. Parameters for other crops are also included. Users will be able to easily incorporate this module into a larger plant simulation model in order to add the ability to simulate photosynthesis. The module is also useful as a teaching aid.

Photosynthesis includes the processes of CO_2 assimilation and water vapor release by plant leaves. It is one of the more important processes for life on Earth as it provides carbohydrate for food and oxygen for respiration. Because plant growth depends on photosynthesis it is an essential building block of plant simulation models. Photosynthesis models range in complexity from correlative models based on radiation use efficiency (Monteith, 1977) where carbon assimilation is proportional to total irradiance absorbed by leaf surfaces to models based on enzyme kinetics (Farquhar et al., 2001).

A coupled approach to photosynthesis-stomatal conductance-transpiration modeling for C_3 plants has been presented by a number of authors (Collatz et al., 1991; Harley et al., 1992; Leuning et al., 1995; Nikolov et al., 1995). This approach combines the FvCB (Farquhar-von Caemmerer-Berry) C_3 photosynthesis model (Farquhar et al., 1980; Farquhar and von Caemmerer, 1981) with a model of stomatal conductance (Ball et al., 1987; Leuning, 1995) and an energy balance equation. The coupled-model approach can describe the photosynthetic behavior of leaves by taking into account the biochemical limitation for CO_2 assimilation (demand) as well as the stomatal limitation to CO_2 (supply), linked to transpiration and canopy temperature. These models describe photosynthesis mechanistically based on its key biochemical and anatomical characteristics. A comprehensive biochemical model for C_4 photosynthesis was developed more recently by von Caemmerer and Furbank (1999).

The parameterization for these models is reasonably stable over a range of environments and practical to carry out. Many of the important parameters can be derived from measurements with portable photosynthesis systems such as LI-COR 6400 (Li-Cor Biosciences, Lincoln, NE, USA). Furthermore, the temperature dependence of photosynthesis and its key enzyme activities has been determined experimentally for both C_3 and C_4 plants (Bernacchi et al., 2001; Kubien, 2003; Kim, 2006, 2007; Massad et al., 2007; Sage and Kubien, 2007). Dubois et al., (2007) discuss methods for statistical estimation of the parameters. Parameters determined using the Li-Cor 6400 and published values were successfully used in a simulation model to estimate field level

maize yields in Maryland, USA (Kim et al., 2012), potato in growth chambers (Fleisher et al., 2010), and greenhouse crops (Kim and Lieth, 2003; Kim et al., 2007b).

Model Descriptions and Governing Equations

The C_3 model:

The basis of this module is the biochemical model for C_3 photosynthesis by Farquhar et al. (1980) as modified by Harley et al. (1992) and de Pury and Farquhar (1997). Photosynthesis in C_3 plants is mathematically abstracted as three processes. These are the rates of carboxylation catalyzed by Rubisco electron transport, and triose phosphate utilization. As irradiance increases, CO_2 fixation becomes less limited by light and more limited by rate of carboxylation governed primarily by Rubisco kinetics (von Caemmerer and Farquhar, 1981, 1982). Similarly, at low CO_2 levels, CO_2 fixation is limited by Rubisco while at higher CO_2 levels, it is limited by RuBP regeneration. Sharkey (1985) identified the rate of triose phosphate utilization (TPU) as the third limiting process in photosynthesis. Harley et al. (1992) implemented the TPU limitation in their model.

The external variables that determine steady state leaf photosynthetic rate include intercepted light, CO_2, temperature and vapor pressure deficit (calculated from relative humidity and temperature). Net CO_2 assimilation rate, A_n , in C_3 plants is assumed to be limited by three processes: Rubisco-catalyzed carboxylation rate [(A_v), regeneration of RuBP (A_j) controlled by electron transport rate, or the triose-phosphate utilization, TPU (A_p). Thus net photosynthetic rate (A_n, μmol CO2 m-2 s-1) is the minimum of A_v, A_j or A_p and can be expressed as:

$$A_n = \min\{A_v, A_j, A_p\} - R_d \qquad 1$$

where R_d is the mitochondrial respiration rate in light or day respiration (for brevity, the units are specified with the variable listing in the appendix).

Rubisco limited photosynthetic rate is calculated as:

$$A_v = V_{c\max} \frac{C_i - \Gamma^*}{C_i + K_c(1 + O/K_o)} \quad (2)$$

where $V_{c\,max}$ is the temperature dependent maximum rate of Rubisco carboxylation, C_i is the intercellular CO_2 partial pressure, O is the partial pressure of oxygen (210 mbars), Γ^* is the CO_2 compensation point in the presence of R_d, K_c is the temperature dependent Michaelis-Menten constant of Rubisco for CO_2, and K_o is the Michaelis-Menten constant of Rubisco for O_2. C_i is calculated as:

$$C_i = C_a - A_n \cdot \left(\frac{1.6}{g_{sw}} + \frac{1.37}{g_b} \right) \cdot P_a \quad (3)$$

where C_a is atmospheric CO_2 content, A_n is net photosynthesis, g_{sw} is stomatal conductance to water vapor, g_b is the boundary layer conductance to water vapor, and P_a is the partial pressure of the atmosphere. In practice, an iterative method is used to solve for C_i using a search algorithm (e.g., secant, bisectional) since A_n is also needed to calculate stomatal conductance as will be described later.

The CO_2 compensation point in the absence of day respiration (Γ^*) is temperature dependent and calculated as:

$$\Gamma^* = 36.9 + 1.88 \cdot (T_L - 25) + 0.036 \cdot (T_L - 25)^2 \quad (4)$$

where T_L is leaf temperature in °C.

RuBP regeneration limited photosynthetic rate (*Aj*) through electron transport is:

$$A_j = \frac{J \cdot (C_i - \Gamma^*)}{4 \cdot (C_i + 2\Gamma^*)} \quad (5)$$

where J is the electron transport rate, and the other variables defined as above. The light dependence of the rate of electron transport, J, can be expressed as:

$$\theta J^2 - (I_a + J_{\max})J + I_a J_{\max} = 0 \quad (6)$$

Where θ is curvature of response of electron transport to photosynthetically active radiation (PAR) , J_{max} is the maximum electron transport rate at the temperature of the leaf, I_2 is PAR effectively absorbed by Photosystem II. The variable I_a is calculated as:

$$I_2 = \alpha I(1-f)/2 \quad (7)$$

Where I is the incident light in photosynthetic flux density (μmol photons m^{-2} s^{-1}) (PFD), α is leaf absorbance in PAR, and f is the spectral correction factor (0.2). The value of J in Eq. [6] is obtained using a quadratic equation.

A_p, the TPU limited photosynthetic rate, is calculated as:

$$A_p = 3 \cdot P_u \quad (8)$$

where P_u is the rate of TPU. An Arrhenius function is used to calculate the temperature dependence of K_c, K_o, R_d, V_{cmax} and P_u. For example,

$$K_c = K_{c25} \exp\left[E_a \cdot (T_L - 25)/\{298 \cdot R \cdot (T_L + 273)\}\right] \quad (9)$$

Where E_a is the activation energy (varies by process), T_L is the leaf temperature, and R is the universal gas constant. Each temperature dependent parameter has a value at 25C, i.e., $K_{c\,25}$,

V_{Cmax25}, etc. Eq. [9] scales the variable for the current leaf temperature as a function of the value at 25 ºC.

The parameter J_{max} in the light dependence function is also temperature dependent and varies as:

$$J_{\max} = J_{m25} \cdot \exp\left[\frac{(T_L - 25)\cdot E_a}{R\cdot(T_L+273)\cdot 298}\right] \cdot \frac{\left[1+\exp\left(\frac{S\cdot 298 - H}{R\cdot 298}\right)\right]}{\left[1+\exp\left(\frac{S\cdot(T_L+273)-H}{R\cdot(T_L+273)}\right)\right]} \quad 10$$

Where E_a and R are as defined above, H is the curvature parameter determining the rate of $J_{\max}$ decrease above the peak temperature, S is the entropy factor.

The leaf age dependence function for J_{max}, V_{cmax} and P_u is given as:

$$f(t) = \max\left[0.0, \frac{t}{t_{opt}}\exp\left(1.0 - \frac{t}{t_{opt}}\right)\right] \quad 11$$

Where t is leaf age (days, physiological age, or GDD), t_{opt} is the optimal age for photosynthesis to peak. This function scales between 0 and 1, and has also been used for scaling final leaf size in response to temperature in maize (Kim et al., 2012).

The C_4 Model:

The biochemical demand for CO_2 assimilation is adapted from von Caemmerer and Furbank (1999). The rate of net CO_2 assimilation (A_n) is represented by the minimum of enzyme limited (A_c) and electron transport limited (A_j) assimilation rates.

$$A_n = \min h\left\{A_c, A_j\right\} \quad 12$$

Where A_c is the enzyme limited CO_2 assimilation rate, and A_j is the electron transport limited CO_2 assimilation rate. The transition between A_c and A_j is calculated using a hyperbolic minimum (*minh*) which is equivalent to taking the lower root of quadratic solution with a curvature factor which may be interpreted as a parameter of co-limitation (Kirschbaum, 1994;

Buckley et al., 2003). A_c can be approximated by the minimum of phosphoenol pyruvate carboxylase (PEPC) and Rubisco activities taking into account the bundle-sheath leakage rate and mitochondrial respiration.

$$A_c = \min\left\{(V_p + g_{bs}C_m - 0.5R_d), (V_{c\max} - R_d)\right\} \quad (13)$$

Where V_p is the rate of C_4 carboxylation, g_{bs} is the bundle sheath conductance to CO_2, C_m is the mesophyll CO_2 partial pressure, and R_d is mitochondrial respiration. In the model, A_c is solved using a quadratic expression as described by von Caemmerer (2000) which was not introduced here for brevity. Provided that the resistance for CO_2 from intercellular spaces to mesophyll cells is negligible, C_m can be estimated by:

$$C_m \cong C_i = C_s - A_n\left(\frac{1.6}{g_s} + \frac{1.37}{g_b}\right) \quad (14)$$

Where C_m and C_i are as defined above, g_s is stomatal conductance, A_n is net carbon assimilation rate, and C_s is the CO_2 concentration at the leaf surface inside the boundary layer. As is done in the C_3 model, an iterative method is used to solve for C_m using a search algorithm since A_n is also needed to calculate stomatal conductance.

The rate of C_4 carboxylation (V_p) is assumed to be limited either by PEPC activity or PEP regeneration.

$$V_p = \min\left\{\frac{C_m V_{p\max}}{C_m + K_p}, V_{pr}\right\} \quad (15)$$

Where V_{pmax} is the maximum PEP carboxylation rate, K_p is the Michaelis-Menton constant for CO_2 of PEPC, and V_{pr} is PEP regeneration rate.

The assimilation rate limited by electron transport (A_j) can be approximated similarly to A_c by the minimum of electron transport limited rates in C_4 and C_3 cycles.

$$A_j = \min\left\{\left(\frac{xJ}{2} - R_m + g_{bs}C_m\right), \left(\frac{(1-x)J}{3} - R_d\right)\right\} \quad 16$$

where J is the electron transport rate, x is a partitioning factor of J, R_m is mitochondrial respiration in the mesophyll, g_{bs} is bundle-sheath conductance to CO_2, R_d is mitochondrial respiration in the light, C_m is as defined above. Total rate of electron transport (J) was modeled using the non-rectangular hyperbolae which can be described as a hyperbolic minimum (*minh*) (Buckley et al., 2003).

$$J = \text{minh}\{I_2, J_{\max}, \theta\} \quad \text{where} \quad \theta J^2 - J(I_2 + J_{\max}) + I_2 J_{\max} = 0 \quad 17$$

Where I_2 is effective radiation absorbed by PSII (Eqn. [7]), θ is curvature of response of electron transport to PAR, and J_{max} is the maximum rate of electron transport.

The temperature dependence of Vp_{max}, Vc_{max}, K_o, K_c, and R_d was approximated by the Arrhenius equation (k_T) normalized at 25 °C.

$$k_T = \exp\left[E_a(T_K - 298)/(298RT_K)\right] \quad 18$$

The temperature dependence of K_p and Vp_r was assumed to be Q_{10} of 2.0. The temperature dependence of J_{max} was modeled using a peaked function (Medlyn, 2002).

$$k_{Tpeak} = k_T\left[1 + \exp\left(\frac{298S - H}{298R}\right)\right]\left[1 + \exp\left(\frac{ST_K - H}{RT_K}\right)\right]^{-1} \quad 19$$

Where H and S are defined as in the C_3 model (Eq.[10]]) and temperature is in Kelvin.

The effect of leaf nitrogen content (N_l in g m^{-2}) on photosynthetic capacity is described using a logistic function (Vos et al., 2005).

$$k_N = \frac{2.0}{1.0 + \exp(-\chi_n(N_l - N_b))} - 1.0 \quad (7)$$

N_b is base N content below which the leaf is non photosynthetic, χ_n determines the rate of change in photosynthesis in response to N_l.

Finally, Vp_{max}, Vc_{max}, and J_{max} were modeled as:

$$V_{p\max} = V_{pm25} \cdot k_N \cdot k_T \quad (20)$$

$$V_{c\max} = V_{cm25} \cdot k_N \cdot k_T \quad (21)$$

$$J_{\max} = J_{m25} \cdot k_N \cdot k_{Tpeak} \quad (22)$$

159

160 *Stomatal Conductance Model*

161 Both the C_3 and C_4 models share the same code for the stomatal conductance (g_s) model. This
162 model is based on the work of Ball et al. (1987) and is called the BWB model. The main form of
163 the conductance model is given as:

$$g_s = g_0 + g_1 \cdot A_n \cdot \frac{h_s}{(C_s / P_a)} \quad (23)$$

164 Where g_0 is residual stomatal conductance to water vapor at the light compensation point in
165 BWB model, g_1 is the empirical coefficient for the sensitivity of g_s to A_n, C_s and h_s; h_s is relative
166 humidity at the leaf surface (as a fraction), A_n is net photosynthesis, C_s is CO_2 concentration at
167 the leaf surface, and P_a is the partial pressure of the atmosphere. C_s is estimated as:

$$C_s = C_a - A_n \cdot \frac{1.37}{g_{bw}} \cdot P_a \quad (24)$$

168

169 Where g_{bw} is boundary layer conductance to water vapor.

170 Boundary layer conductance (g_{bw}) in relation to wind speed (u) and leaf dimension (d) is:

$$g_{bw} = 0.147\sqrt{\frac{u}{d}} \quad (25)$$

$$d = 0.72 \cdot w$$

171 Where w is leaf width (m).

172 A quadratic equation is used to obtain h_s by combining g_s with the diffusion equation (Eq. [24])

$$a_h \cdot h_s^2 + b_h \cdot h_s + c_h = 0 \qquad 26$$

$$\text{where} \begin{cases} a_h = \dfrac{g_1 \cdot A_n}{C_s} \\ b_h = g_0 + g_{bw} - \left(g_1 \cdot A_n / C_s\right) \\ c_h = \left(-h_a \cdot g_{bw}\right) - g_0 \end{cases}$$

173 And g_0, g_1 and g_{bw} are defined as above. The vapor pressure deficit, D_s, at the leaf surface is
174 given as:

$$D_s = \left(1 - h_s\right) \cdot e_s \qquad 27$$

175 Where e_s is vapor pressure at the leaf surface (assumed saturated).

176 Leaf temperature, T_L, is determined using a linearized solution (Norman and Campbell, 1998) of
177 the energy budget equation for temperature at the leaf surface:

$$T_L = T_a + \frac{\gamma^*}{s + \gamma^*}\left[\frac{R_{abs} - \varepsilon \cdot \sigma \cdot T_a^4}{g_{hr} c_p} - \frac{D}{p_a \gamma^*}\right] \qquad 28$$

$$\gamma^* = \frac{\gamma \cdot g_{hr}}{g_v}$$

$$g_{hr} = g_h + g_r$$

178 Where T_a is air temperature, R_{abs} is absorbed long-wave and short-wave radiation per surface leaf
179 area, ε is leaf thermal emissivity (set to 0.97), σ is the Stefan-Boltzmann constant (5.67x 10-8
180 Watts m^{-2} K^{-4}), D is vapor pressure deficit, s is the slope of the slope of the vapor pressure
181 deficit-temperature curve Δ divided by atmospheric pressure:

$$s = \frac{\Delta}{p_a} \qquad 29$$

$$\Delta = \frac{d(e_s)}{dT} = \frac{e_s(T) \cdot 17.502 \cdot 240.97}{\left(c + T\right)^2}$$

182 γ is the psychrometric constant (6.66 x 10^{-4}). Total water vapor conductance per surface leaf area,
183 g_v, is calculated as:

$$g_v = 0.5\frac{g_s \cdot g_{bw}}{g_s + g_{bw}} \quad (30)$$

Heat conductance for the boundary layer is:

$$g_h = \frac{0.135}{0.147} \cdot g_{bw} \quad (31)$$

Radiative conductance is:

$$g_r = \frac{4 \cdot \varepsilon \cdot \sigma \cdot T_L^3}{C_p} \quad (32)$$

Saturated water vapor pressure at temperature (T) is:

$$e_s(T) = 0.611 \cdot \exp\left(\frac{17.502 \cdot T}{240.97 + T}\right) \quad (33)$$

Where T is temperature.

Transpiration rate, E, is calculated as:

$$E = 2 \cdot g_v \cdot \left(\frac{e_s(T_L) - e_a}{P_a}\right) \quad (34)$$

Where all variables are defined as before.

Coupling Photosynthesis and Transpiration

The C_3 and C_4 photosynthesis models use light, CO_2, air temperature, and relative humidity as environmental input variables. Since photosynthetic rate is necessary to calculate stomatal conductance, leaf temperature and C_i or C_m, an iterative method is used to arrive at a solution (Fig. 1). The BWB model requires the net photosynthetic rate (A_n) as an input (Eq. [1] for C_3 and Eq. [12] for C_4), while Ci or C_m results from the interaction of A_n and g_s (Eqs. [3] and[14]). Leaf temperature is estimated from a linear solution of the energy budget equation (Eq. 28]) using air temperature (T_a), and the conductances for heat (g_h) and water vapor (g_v) as input variables. The

diffusion equation is used to relate C_a, C_s and C_i using A, g_s and g_b [Eqns. [3] and [14] for the C_3 and C_4 models respectively, and [26]). Therefore, the three sub-models (photosynthesis, stomatal conductance, and energy balance) are interdependent. A nested iterative procedure was used to solve this relation numerically (Fig. 1). Initially, leaf temperature and C_i were assumed to be equal to T_a and 0.7 C_a, respectively, so as to obtain an estimate of A_n. The estimate of A_n is then used to obtain g_s. C_i was estimated using the resulting A_n and g_s (Eqns. [3] and [14] depending on the model). This process is solved iteratively using the Newton-Raphson method until C_i was stable. Subsequently, leaf temperature is computed using T_a and g_s (Eq. [28]) and compared with the initial leaf temperature. When the new leaf temperature agreed to within 0.1 °C with the initial value, the iteration was assumed to have converged.

Parameterization

We used a stepwise calibration of individual components of the photosynthesis model rather than fitting all parameters simultaneously (Kim and Lieth, 2003; Kim, 2006, 2007). That is, the photosynthetic parameters (V_{cm25}, J_{m25}, R_{d25}) were first determined by fitting the biochemical model of photosynthesis (Farquhar et al., 1980) to the A/C_i response using measured C_i at controlled steady state conditions where PAR is fixed (typically 1500 $\mu mol \cdot m^{-2} \cdot s^{-1}$), and relative humidity and leaf temperature controlled to around 50%, and 25 °C respectively. In addition, V_{cmax} and J_{max} were estimated for individual leaves over a range of temperatures (usually growth temperatures). Temperature dependence of V_{cmax} and J_{max} were then determined by fitting Eqs. [18]- [22]. Temperature dependence of P_u can be determined by fitting Eq. [8] with the net photosynthesis data collected between 10 to 20 °C at 1500 $\mu mol \cdot mol^{-1}$ of CO_2 and 1500 $\mu mol \cdot m^{-2} \cdot s^{-1}$ of PAR, assuming that A_n was primarily governed by the rate of TPU when temperature is low while CO_2 and light are not limiting (Sharkey, 1985). P_{u25} was estimated for the rose data by extrapolating Eq. [9] to 25 ºC (see Fig. 3c in Kim and Lieth, 2003). Temperature

dependencies of K_c, K_o, Γ^*, and R_d were adopted from de Pury and Farquhar (1997), assuming that those parameters were invariant across species. The parameter values of the stomatal conductance model also come from gas exchange data. No parameter values in the energy balance equation are specifically calibrated. The parameterization data included a range of CO_2 concentrations, relative humidities, PAR levels, and temperatures including those conditions where A might approach zero (PAR < 50 $\mu mol \cdot m^{-2} \cdot s^{-1}{}_a{}^{-1}$. Specific details on parameterizing the model for other crops can be found in Kim and Lieth (2003) for rose, Fleisher et al. (2010) for potato, Kim et al. (2007b) for *Scaevola*, and Kim et al. (2012) for garlic. More details on parameterizing the FvCB model in general can be found in Dubois et al. (2007).

Validation of the Module Code

The biochemical models of photosynthesis for both C_3 and C_4 plants have been studied extensively and results have been published in a number of studies (Lenz et al., 2010; Fleisher et al., 2010; Massad et al., 2007; Kim and Lieth, 2003;Kim et al., 2006, 2007). The goal of the validation for this paper is to ensure that the equations for the model have been implemented correctly in the computer code and that the published parameters will give realistic results. This version of the code has been parameterized and tested for Rose (*Rosa hybrida* L.) by Kim and Lieth (2003), potato by Fleisher et al. (2010) and corn by Kim et al. (2006, 2007). Some of the simulations for Rose are repeated here to show that the current version of the code for C_3 crops gives similar results as those published by Kim and Lieth (2003). Simulations for net photosynthesis response to light, internal CO_2 and leaf temperature for Rose are shown in Figures 2a, 2b, and 2c. The responses and errors are similar to those shown in Kim and Lieth (2003). Note that the measurement errors for leaf temperature are higher than those for CO_2 and light response. This is because it is difficult to control leaf temperature in the LiCor 6400 chamber.

Figure 3 shows a CO_2 response curve for potato estimated by the photosynthesis module for the calibration data from Fleisher et al (2010). Figure 4 shows CO_2 and light response curves for potato grown in sunlit growth chambers in a later study from unpublished data. The same parameters from Fleisher et al. (2010) were used from these simulations. Figure 5 shows estimated and observed leaf level transpiration as a function of stomatal conductance from leaves from the same unpublished data. The simulated values are slightly greater than observed at higher values of stomatal conductance. Since transpiration is affected by other variables in addition to stomatal conductance there tends to be more variance in the observed and simulated values. Also, the stomatal conductance submodel has not been calibrated to the same extent as the photosynthesis model.

Net photosynthesis data for maize as a function of internal CO_2 concentration (C_i) is shown in Figure 6. The parameters for the C_4 corn model were calibrated data reported in Kim et al. (2006 and 2007). The observed data in this figure were taken from corn grown in a field experiment in Beltsville, MD, U.S.A in 2002 and may have been subject to water stress. Note the shape of the curve and photosynthetic rates simulated by the model are within the range of the measured data. The corn model was calibrated under optimum growing conditions for corn as was present in the growth chambers. As a result, the net photosynthesis rates were in the high range as compared to other publications. Massad et al. (2007) in a study on C_4 model parameters noted that leaf photosynthesis rates for corn can be variable due to different growing conditions and stresses that may occur. It should be noted that the errors are largest at maximal light levels. At the canopy level, not all the leaves will be light saturated. As a result the errors of maximal photosynthesis may not translate to large errors for canopy level photosynthesis where light levels vary over time and over canopy position. Figure 7 shows simulated net photosynthesis and transpiration as a function of PAR. The data for this figure come from a field experiment carried out in Beltsville, MD, U.S.A in 2002 (unpublished). Note that the variability mainly occurs at high light or internal CO_2 levels. Again net photosynthesis is estimated well at all light levels but the simulated values range toward the high end. The differences for ET are larger at the high light

278 levels. Again, the model has not been extensively calibrated and tested for the stomatal
279 conductance submodel.

280

281 **Scaling to Canopy Level**

282 The coupled leaf physiology model can be scaled to estimate canopy level values of
283 photosynthesis and transpiration. One approach is to calculate the light and temperature regime
284 for individual leaves in the canopy depending on their location in the canopy and aggregating
285 leaf level photosynthesis rates over the canopy. A simpler approach is to divide the canopy into
286 sunlit and shaded components (de Prury and Farquhar, 1997) and calculate gas exchange rates
287 for each component and sum them. Canopy level gas exchange rates have been calculated using
288 this method for sunlit growth chamber grown plants by Kim et al (2007) for corn and Fleisher et
289 al. (2010) for potato. The code has also been used to estimate dry matter and leaf area
290 production of corn grown under field conditions (Kim et al., 2012).

291

292 **Conclusions and Further Applications**

293

294 The comprehensive model described here that couples key leaf gas exchange processes is a
295 critical tool in plant physiological and ecological research. This model can be used to evaluate
296 the interactions between plants and the environment, and to forecast global carbon and water
297 budgets in response to climate change. Because the gas exchange processes are not only sensitive
298 to the microclimate surrounding the plant canopy but also closely related to soil and root
299 processes in addition to endogenous biochemical regulations, a leaf gas exchange model should
300 account for the interrelationships among carbon, water and nitrogen economies of above and
301 below ground parts. That is, the model needs account for biochemical demand for CO_2
302 assimilation, physical supply of CO_2 and loss of water through stomata, supply of water from the

soil through transpiration stream, and stomatal control to balance these interrelated processes. Consequently, such model should also account for soil water status. In addition, the dependence on leaf physiological status like water potential, nitrogen content and age, which are key determinants of plant performance, should be also accounted for. This can be accomplished by numerically combining the component models of photosynthesis, stomatal conductance, and energy balance as described here and their response functions to various conditions. Such response functions have not been included here but the reader can find a number of them in the literature. For example, the Tardieu-Davies (TD) model of stomatal regulation as a function of Abscisic acid (ABA) concentration (Tardieu and Davies, 1993) has been used to model stomatal response to water stress. The TD model has been used in conjunction with the BWB model (Dewar, 2002; Gutschick, 2002).

References

Ball J.T., Woodrow I.E., Berry J.A. 1987. A model predicting stomatal conductance and its contribution to the control of photosynthesis under different environmental conditions. In: Biggens J, ed. Progress in photosynthesis research. The Netherlands: Martinus Nijhoff Publishers.

Bernacchi, C. J., Singsaas, E. L., Pimentel, C., Portis Jr, A. R., and Long, S. P. 2001. Improved temperature response functions for models of Rubisco-limited photosynthesis. Plant, Cell & Environment. 24:253-259.

Buckley, T. N., Mott, K. A., and Farquhar, G. D. 2003. A hydromechanical and biochemical model of stomatal conductance. *Plant, Cell and Environment*. 26:1767-1785.

Campbell, G.S., and J.M. Norman. 1998. The light environment of plant canopies. An Introduction to Environmental Biophysics. Springer, New York. pp: 247-281.

Collatz G.J., Ball J.T., Grivet C., Berry J.A. 1991. Physiological and environmental regulation of stomatal conductance, photosynthesis and transpiration: a model that includes a laminar boundary layer. Agricultural and Forest Meteorology 54:107-136

de Pury, D.G. and Farquhar G.D. 1997. Simple scaling of photosynthesis from leaves to canopies without the errors of big-leaf models. Plant, Cell and Environment 20: 537-557.

Dubois, Jean-Jacques B., Fiscus, Edwin L., Booker, Fitzgerald L., Flowers, Michael D., and Reid, Chantal D. 2007. Optimizing the statistical estimation of the parameters of the Farquhar-von Caemmerer-Berry model of photosynthesis. *New Phytologist*. 176:402-414.

Farquhar GD, von Caemmerer S, Berry J.A. 1980. A biochemical model of photosynthetic CO2 assimilation in leaves of C3 species. Planta 149: 78±90.

Farquhar, G.D., von Caemmerer, S. (1981) Modelling of photosynthetic response to environmental conditions. In: Physiological plant ecology, Vol. 12 B: Water relations and photosynthetic productivity, Lange, O.L., Nobel, P.S., Osmond, C.B., Ziegler, H., eds., Springer-Verlag, Berlin Heidelberg New York.

Farquhar, Graham D., von Caemmerer, Susanne, and Berry, Joseph A. 2001. Models of Photosynthesis. *Plant Physiol.* 125:42-45.

Fleisher, D.H., D.J. Timlin, Y. Yang, and V.R. Reddy. Simulation of potato gas exchange rates using SPUDSIM. Agric. and Forest Met. 150:432-442. 2010.

Harley P. C., Thomas R. B., Reynolds J. F., Strain B. R. 1992. Modelling photosynthesis of cotton grown in elevated CO2. Plant, Cell and Environment 15:271-282.

Kim, S.-H., and J. H. Lieth. 2003. A coupled model of photosynthesis, stomatal conductance and transpiration for a rose leaf (*Rosa hybrida* L.). Ann. Bot. 91:771–781.

Kim, S.-H., P.R. Fisher, and J.H. Lieth, 2007. Analysis and modeling of gas exchange processes in *Scaevola aemula*. Scientia Horticulturae 114:170-176.

Kim, S.-H., D.C. Gitz, R.C. Sicher, J.T. Baker, D.J. Timlin, and V.R. Reddy. 2007. Temperature dependence of growth, development, and photosynthesis in maize under elevated CO2. Env. Exp. Bot. 61:224-236.

Kim, S.-H., J.H. Jeong, and L.L. Nackley, 2012. Characterization and modeling of photosynthetic responses to light, CO2, temperature, and leaf nitrogen in garlic. Journal of American Society for Horticultural Science (in review).

Kim, S.-H., R.C. Sicher, H. Bae, D.C. Gitz, J.T. Baker, D.J. Timlin, and V.R. Reddy. 2006. Canopy photosynthesis, evapotranspiration, leaf nitrogen, and transcription profiles of maize in response to CO_2 enrichment. Global Change Biology 12:588-600.

Kim, S-H, Y. Yang, D.J. Timlin, D. Fleisher, A. Dathe, V.R. Reddy. 2012. Modeling Nonlinear Temperature Responses of Leaf Growth, Development, and Biomass in MAIZSIM. Agron. J. 104:1523-1537.

Kirschbaum, M., 1994. The sensitivity of C_3 photosynthesis to increasing CO_2 concentration: a theoretical analysis of its dependence on temperature and background CO_2 concentration. Plant, Cell Environ. 17, 747–754.

Kubien, D.S., von Caemmerer, S., Furbank, R.T., Sage, R.F., 2003. C_4 photosynthesis at low temperature. A study using transgenic plants with reduced amounts of Rubisco. Plant Physiol. 132 (3), 1577–1585.

Lenz, K.E., G. E. Host, K. Roskoski, A. Noormets, A. Sôber, D. F. Karnosky. 2010. , 2010. Analysis of a Farquhar-von Caemmerer-Berry leaf-level photosynthetic rate model for Populus tremuloides in the context of modeling and measurement limitations. Environmental Pollution. 158:1015 - 1022

Leuning R, Kelliher FM, de Pury DGG, Schulze E-D. 1995. Leaf nitrogen, photosynthesis, conductance and transpiration: scaling from leaves to canopies. Plant, Cell and Environment 18: 1183-1200.

Leuning R. 1995. A critical appraisal of a combined stomatal photosynthesis model for C_3 plants. Plant, Cell and Environment 18: 339:355.

Massad, Raia-Silvia, Tuzet, Andres, and Bethenod, Olivier. 2007. The effect of temperature on C_4-type leaf photosynthesis parameters. Plant, Cell & Environment. 30:1191-1204.

Monteith, JL. 1977. Monteith, JL,(1977). Climate and efficiency of crop production in Britain. *Phil. Trans. R. Soc. London, B*. 281:277-294.

Nikolov NT, Massman WJ, Shoettle AW. 1995. Coupling biochemical and biophysical processes at the leaf level: an equilibrium photosynthesis model for leaves of C3 plants. Ecological Modelling 80: 205-235.

Sharkey TD. 1985. Photosynthesis in intact leaves of C3 plants: physics, physiology and rate limitations. Botanical Review 51:53-105.

Tardieu, F. and Davies, W. J. 1993. Integration of hydraulic and chemical signalling in the control of stomatal conductance and water status of droughted plants. Plant, Cell & Environment. 16:341-349.

von Caemmerer S., and Farquhar G. D. 1981. Some relationships between the biochemistry of photosynthesis and the gas exchange of leaves. Planta 153:376–387

von Caemmerer S. and Furbank R. T. 1999. The modelling of C4 photosynthesis. In: Sage RF and Monson RK (eds) C_4 Plant Biology, pp 173–211. Academic Press, San Diego, California

von Caemmerer, S., 2000. Biochemical models of leaf photosynthesis. CSIRO Publishing, Collingwood, Australia.

Wullschleger, S. D. 1993. C_3 plants – A retrospective analysis of the A/Ci curves from 109 species. Journal of Experimental Botany 44: 907–920.

Figure Captions

Figure 1. Flow chart for the model (from Kim and Lieth, 2003)

Figure 2. Simulated and observed carbon assimilation rates as a function of light (a), internal CO_2 concentration (b), and leaf temperature (c) in Rose (*Rosa hybrida* L.) from Kim and Lieth (2003).

Figure 3. Simulated and observed carbon assimilation rates for potato (*Solarium tuberosum* L.) as a function of internal CO_2 concentration. These are calibration data from Fleisher et al. (2010).

Figure 4. Simulated and observed carbon assimilation rates for potato as a function of internal CO_2 concentration (a) and light (b) using parameters from the data in Figure 3.

Figure 5. Simulated and observed transpiration rates for potato as a function of stomatal conductance .

Figure 6. Simulated and observed carbon assimilation rates for maize (Zea Mays L.) as a function of internal CO_2 concentration.

Figure 7. Simulated and observed carbon assimilation rates (a) and transpiration (b) as a function of light for maize.

420

421 **Appendix A. Variable names and description.**

422

Variables, parameters, and their values used in the model. The values with the superscript 'a' are from de Pury and Farquhar (1997). All parameters are projected leaf area basis unless stated otherwise.

Symbol	Value	Units	Description
Photosynthesis model			
Γ	-	μbar	CO_2 compensation point in the presence of R_d
Γ^*	-	μbar	CO_2 compensation point in the absence of R_d
ξ	-	day	Leaf age counted as days after unfolding
θ	0.7[a]	-	Curvature of response of electron transport to PAR
δ	0.15	-	Leaf reflectance plus transmittance
A_n	-	$\mu mol \cdot m^{-2} \cdot s^{-1}$	Net CO_2 assimilation rate (photosynthetic rate)
A_c	-	$\mu mol \cdot m^{-2} \cdot s^{-1}$	Rubisco limited CO_2 assimilation rate
A_j	-	$\mu mol \cdot m^{-2} \cdot s^{-1}$	Electron transport limited CO_2 assimilation rate
A_{max}	-	$\mu mol \cdot m^{-2} \cdot s^{-1}$	Light saturated CO_2 assimilation rate at ambient $[CO_2]$

A_p	-	μmol·m^{-2}·s^{-1}	Triose phosphate utilization limited CO_2 assimilation rate (C3 model only)
C_i	-	μbar	Intercellular CO_2 partial pressure (C3 model only)
C_m	-	μbar	Mesophyll CO_2 partial pressure (C4 model only)
d_0	1.296	-	Scaling factor of leaf age effect
d_1	0.1468	-	Empirical coefficient to determine growth of leaf age effect
d_2	0.0103	-	Empirical coefficient to determine downward slope of leaf age effect
E_a	-	kJ·mol^{-1}	Activation energy
f	0.15[a]	-	Spectral correction factor
g_{bs}	0.003	μmol m^2 s^1	Bundle sheath conductance to CO_2, mol m^2 s^1
H	219.4	kJ·mol^{-1}	Curvature parameter of the temperature dependence of J_{max}
I	-	μmol quanta·m^{-2}·s^{-1}	Incident PAR (Photosynthetically Active Radiation)
J	-	μmol electrons·m^{-2}·s^{-1}	Electron transport rate
J_{m25}	- 162.0	μmol·m^{-2}·s^{-1}	Potential rate of electron transport at 25 °C

J_{Max}		$\mu mol \cdot m^{-2} \cdot s^{-1}$	Maximum rate of electron transport when temperature is at the optimum
K_{c25}	404[a]	μbar	Michaelis-Menten constant of Rubisco for CO_2
K_{o25}	248[a]	mbar	Michaelis-Menten constant of Rubisco for O_2
O	205[a]	mbar	Oxygen partial pressure
P_{u25}	11.55	$\mu mol \cdot m^{-2} \cdot s^{-1}$	Rate of tirose phosphate utilization at 25 °C
R	8.314	$J \cdot mol^{-1} \cdot K^{-1}$	Universal gas constant
R_{d25}	1.260	$\mu mol \cdot m^{-2} \cdot s^{-1}$	Mitochondrial respiration in the light at 25 °C
S	704.2	$J \cdot mol^{-1} \cdot K^{-1}$	Electron transport temperature response parameter
T_L	-	°C	Leaf temperature
V_c	-	$\mu mol \cdot m^{-2} \cdot s^{-1}$	Carboxylation rate
V_{cm25}	102.4	$\mu mol \cdot m^{-2} \cdot s^{-1}$	Photosynthetic Rubisco capacity at 25 °C
V_{cmax}	-	$\mu mol \cdot m^{-2} \cdot s^{-1}$	Maximum rate of rubisco carboxylation

V_{pmax}	-	$\mu mol \cdot m^{-2} \cdot s^{-1}$	Maximum PEP carboxylation rate (C4 model only)
V_{pr}	-	$\mu mol \cdot m^{-2} \cdot s^{-1}$	PEP regeneration rate (C4 model only)
V_o	-	$\mu mol \cdot m^{-2} \cdot s^{-1}$	Oxygenation rate
Variables with temperature dependence			
K_c	-	$\mu mol \cdot m^{-2} \cdot s^{-1}$	Michaelis-Menten constant of rubisco for CO_2
K_o	-	$\mu mol \cdot m^{-2} \cdot s^{-1}$	Michaelis-Menten constant of rubisco for O_2
P_u	-	$\mu mol \cdot m^{-2} \cdot s^{-1}$	Triose phosphate utilization rate (C3 model only)
K_p		$\mu mol \cdot m^{-2} \cdot s^{-1}$	Michaelis-Menten constant for CO_2 of PEPC
R_d	-	$\mu mol \cdot m^{-2} \cdot s^{-1}$	Mitochondrial respiration in the light
Stomatal conductance model			
g_0	0.0960-	$mol \cdot m^{-1} \cdot s^{-1}$	Minimum stomatal conductance to water vapor at the light compensation point in BWB model
g_1	-	-	
C_a	-	µbar	Ambient CO_2 partial pressure

C_s	-	μbar	CO_2 partial pressure at the leaf surface
g_b	-	$mol \cdot m^{-2} \cdot s^{-1}$	Boundary layer conductance to water vapor
g_s	-	$mol \cdot m^{-2} \cdot s^{-1}$	Stomatal conductance to water vapor
h_a	-	-	Relative humidity of the ambient air
h_s	-	-	Relative humidity at the leaf surface
m	10.055	-	Empirical coefficient for the sensitivity of g_s to A, C_s and h_s in BWB model

Energy balance model

ε	0.97	-	Leaf thermal emissivity
σ	5.67×10^{-8}	$W \cdot m^{-2} \cdot K^{-4}$	Stefan-Boltzmann constant per surface area
λ	44.0	$kJ \cdot mol^{-1}$	Latent heat of vaporization at 25 °C
C_p	29.3	$J \cdot mol^{-1} \cdot C^{-1}$	Specific heat of air
D	-	kPa	Vapor pressure deficit of the ambient air
D_s	-	kPa	Vapor pressure deficit at the leaf surface
E	-	$mol \cdot m^{-2} \cdot s^{-1}$	Transpiration rate per projected leaf area
e_a	-	kPa	Vapor pressure in the ambient air

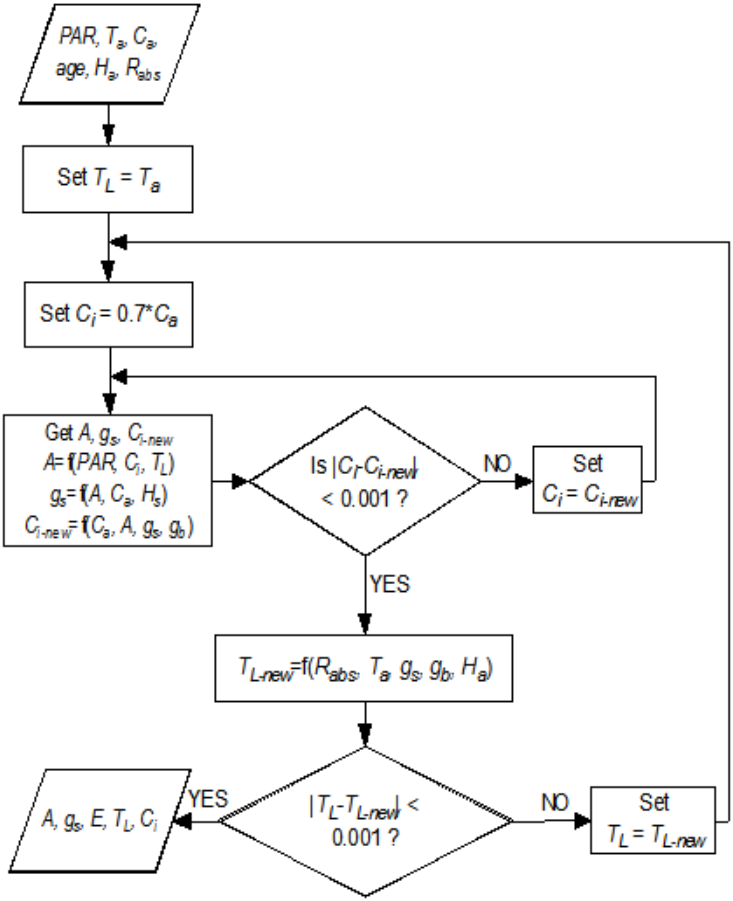
PAR, T_a, C_a, age, H_a, R_{abs}
Set $T_L = T_a$
Set $C_i = 0.7 * C_a$
Get A, g_s, $C_{i\text{-}new}$
$A = f(PAR, C_i, T_L)$
$g_s = f(A, C_a, H_s)$
$C_{i\text{-}new} = f(C_a, A, g_s, g_b)$
Is $|C_i - C_{i\text{-}new}| < 0.001$?
NO
Set $C_i = C_{i\text{-}new}$
YES
$T_{L\text{-}new} = f(R_{abs}, T_a, g_s, g_b, H_a)$
$|T_L - T_{L\text{-}new}| < 0.001$?
YES
NO
Set $T_L = T_{L\text{-}new}$
A, g_s, E, T_L, C_i

Figure 1

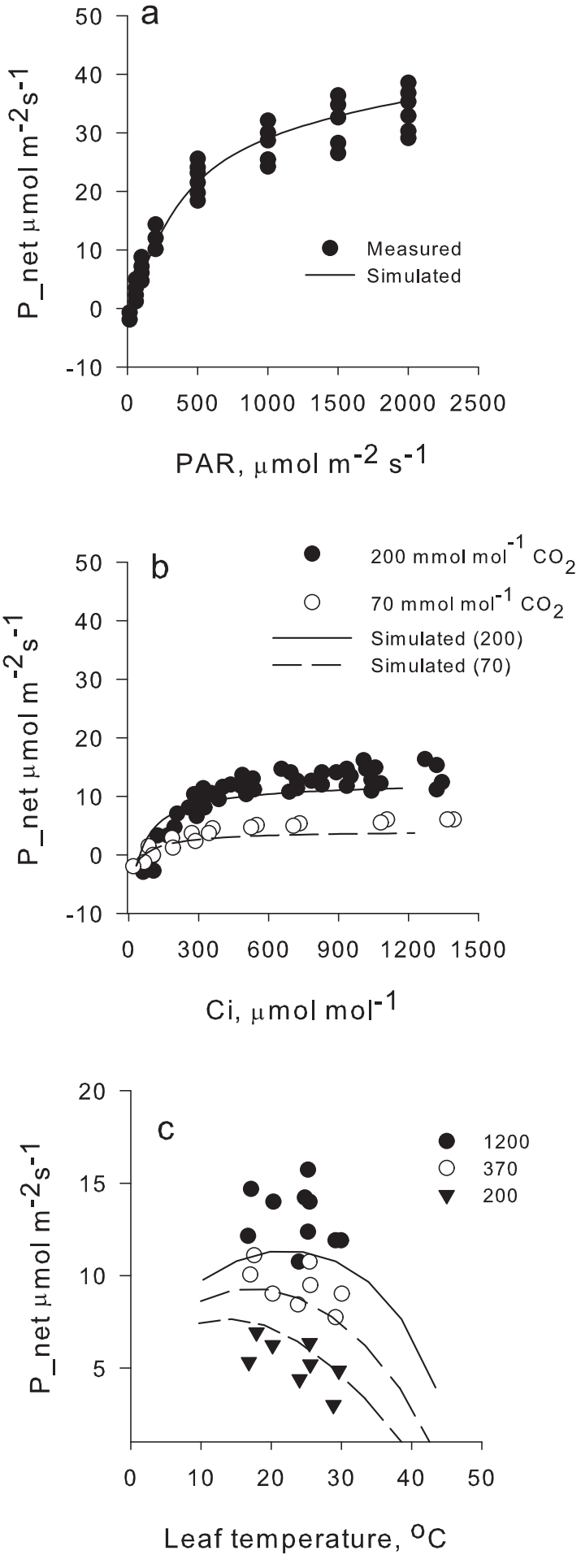
a
50
40
30
20
10
0
-10
P_net µmol m-2s-1
0
500
1000
1500
2000
2500
PAR, µmol m-2 s-1
Measured
Simulated
b
200 mmol mol-1 CO2
70 mmol mol-1 CO2
Simulated (200)
Simulated (70)
50
40
30
20
10
0
-10
P_net µmol m-2s-1
0
300
600
900
1200
1500
Ci, µmol mol-1
c
20
15
10
5
P_net µmol m-2s-1
1200
370
200
0
10
20
30
40
50
Leaf temperature, oC

Figure 2

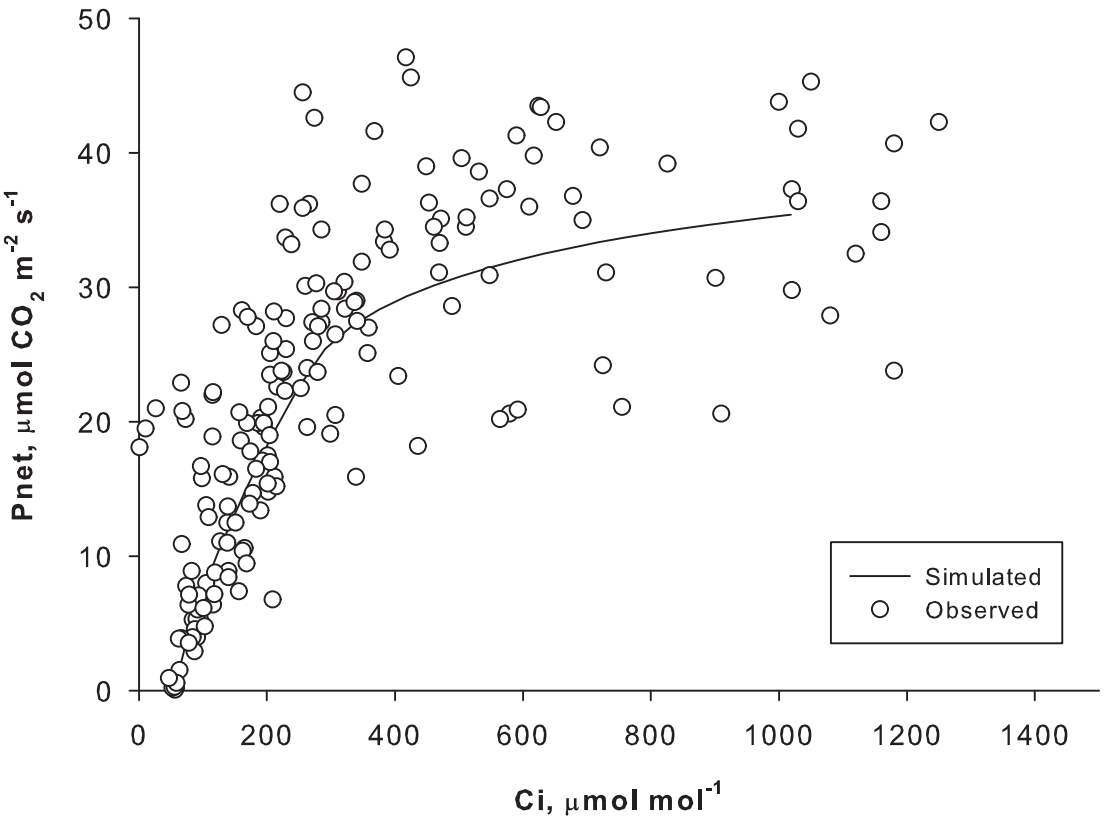
50
40
30
20
10
0
0
200
400
600
800
1000
1200
1400
Pnet, μmol CO2 m-2 s-1
Ci, μmol mol-1
Simulated
Observed

Figure 3

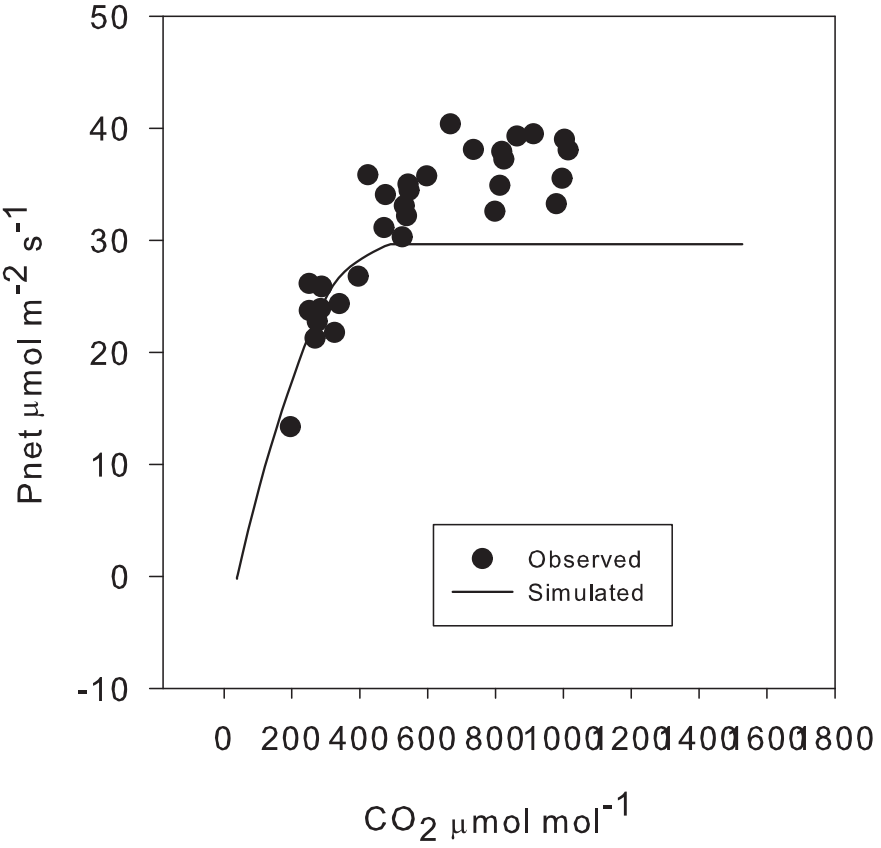
50
40
30
20
10
0
-10
Pnet μmol m-2 s-1
0 200 400 600 800 1000 1200 1400 1600 1800
CO2 μmol mol-1
Observed
Simulated

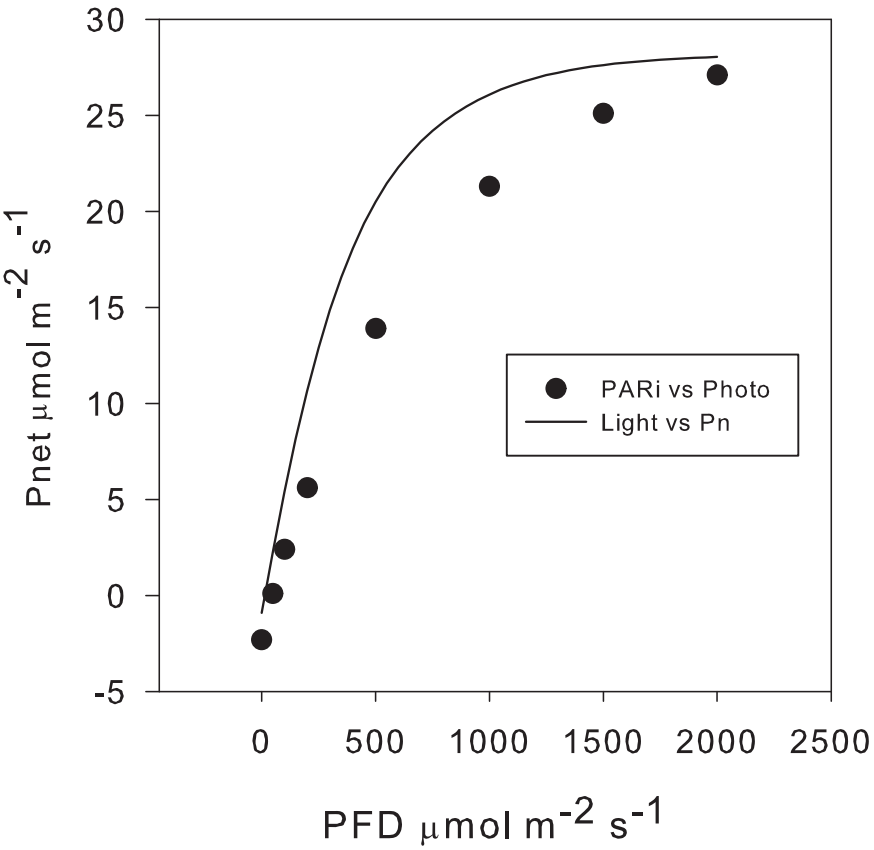
30
25
20
15
10
5
0
-5
Pnet μmol m-2 s-1
0 500 1000 1500 2000 2500
PFD μmol m-2 s-1
PARi vs Photo
Light vs Pn

Figure 4

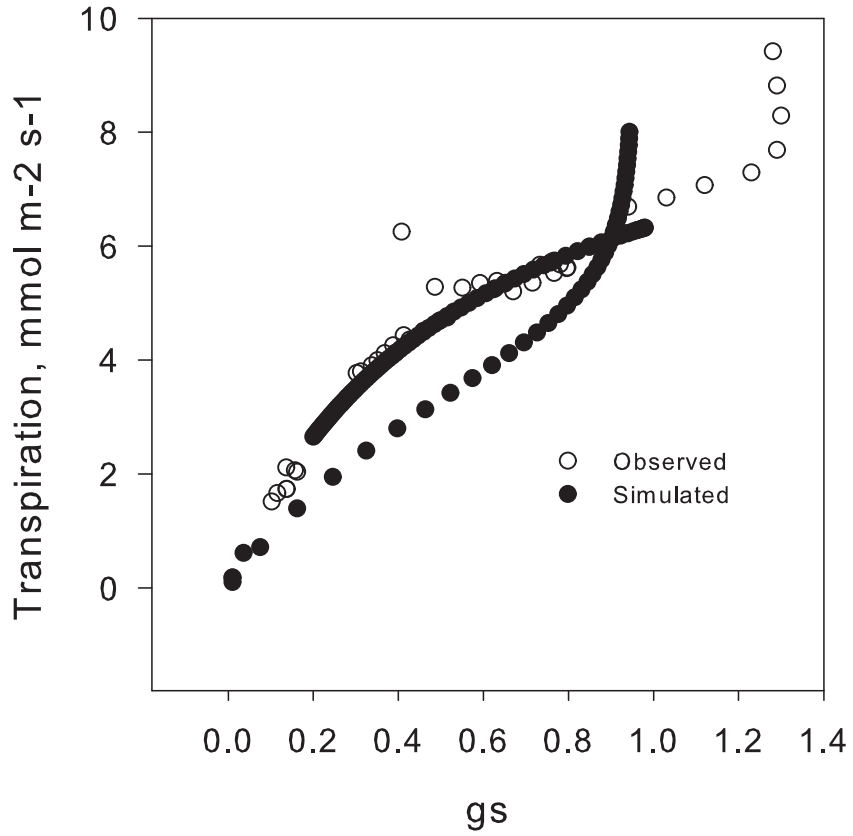
Transpiration, mmol m-2 s-1
10
8
6
4
2
0
0.0
0.2
0.4
0.6
0.8
1.0
1.2
1.4
gs
Observed
Simulated

Figure 5

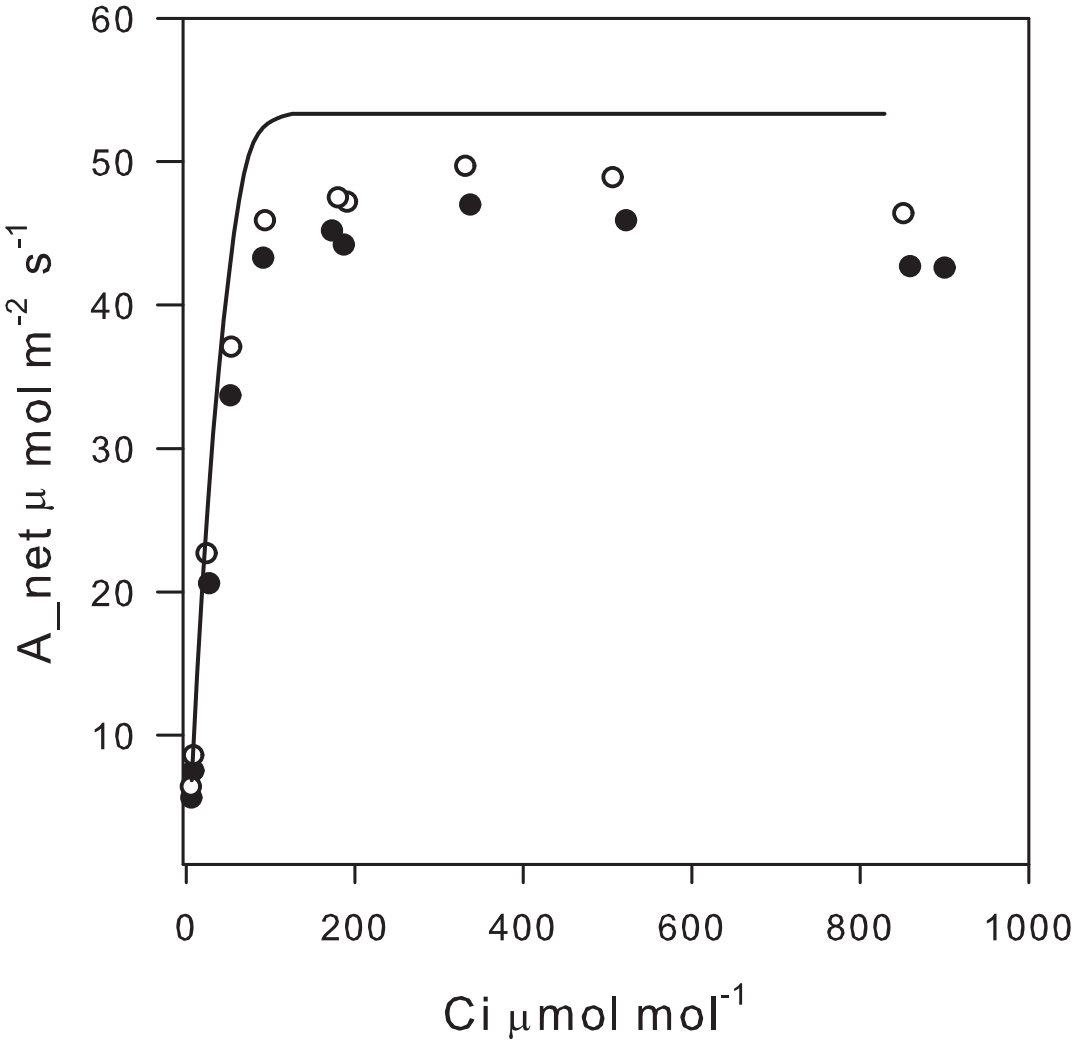
60
50
40
30
20
10
A_net μ mol m-2 s-1
0
200
400
600
800
1000
Ci μmol mol-1

Figure 6

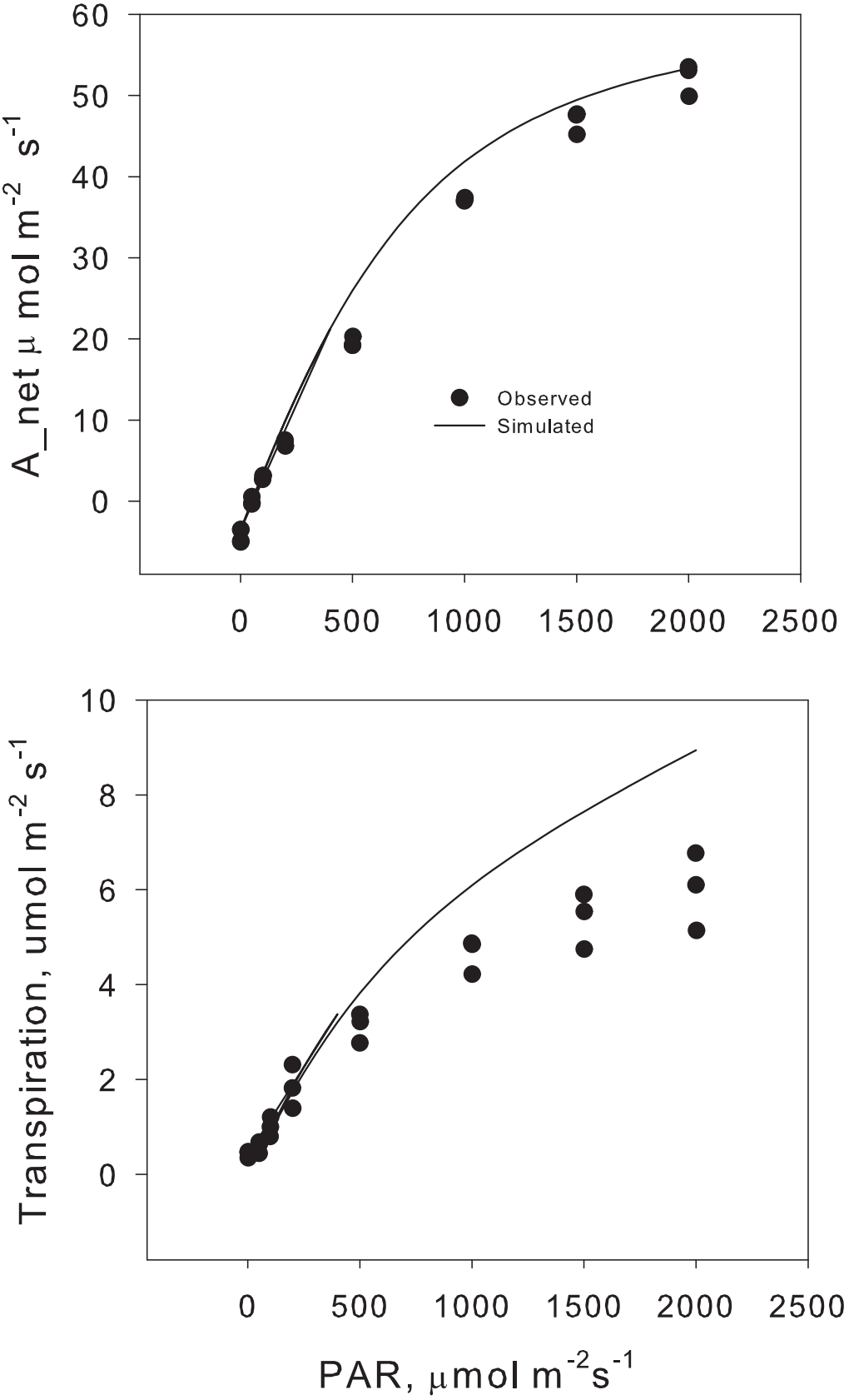
A_net μ mol m-2 s-1
60
50
40
30
20
10
0
0
500
1000
1500
2000
2500
Observed
Simulated
Transpiration, umol m-2 s-1
10
8
6
4
2
0
0
500
1000
1500
2000
2500
PAR, μmol m-2s-1

Figure 7